

assembly. It means that if a location rather than the end of slab is considered, the time for ‘b’ would come much later, depending on the progress of the interface in the LP. Eventually, small pore is invaded by air at around 55,700 sec, indicated in Fig. 5. as ‘c’. This moment can be considered as the end of funicular stage for this considered location as the liquid phase becomes isolated (Fig. 4b), and possibly the beginning of pendular stage, where the presence of liquid would be limited to the liquid bridges between solid particles.

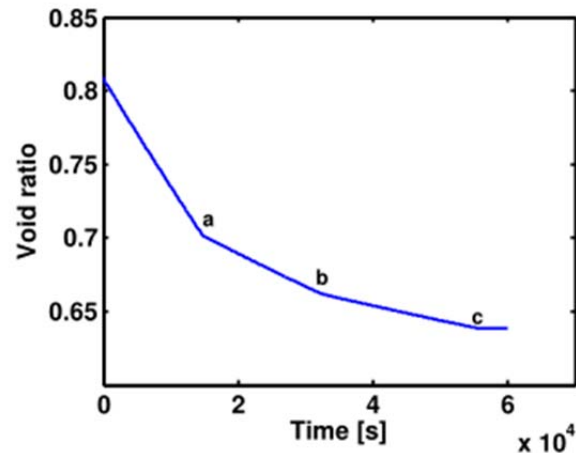


Fig. 6. Evolution of void ratio simulated.

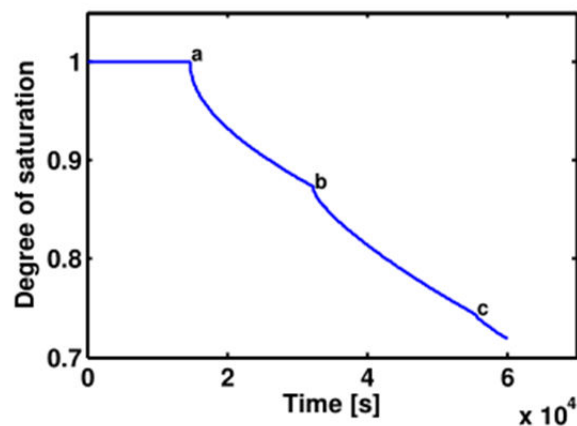


Fig. 7. Evolution of degree of saturation simulated.

The initial void ratio and volumetric water content are calibrated against experimental data reported in Peron et al. (2009) and Hu et al. (2013c). Fig. 8 shows the correlation between void ratio and volumetric water content. It should be pointed out that the characteristic moments in presented model are different from those in the previous 1D model, the latter result from homogenization of the entire soil slab while the former have to be considered locally and are distinctly different at different locations. Consequently, one characteristic moment in the 1D model, the end of the full desaturation of LP cannot be applied here. It is interesting to note that the drying rate (loss of volumetric water content) is very high throughout the process. It has been established that the drying rate would experience a decrease in the “falling rate

period” after the initial “constant rate period” (e.g. Sherwood 1929). Macroscopic modeling has successfully reproduced this observation (e.g. Puyate and Lawrence 2006). The present model most likely can be better calibrated and provide the corresponding scenario developed at the micro and meso scales.

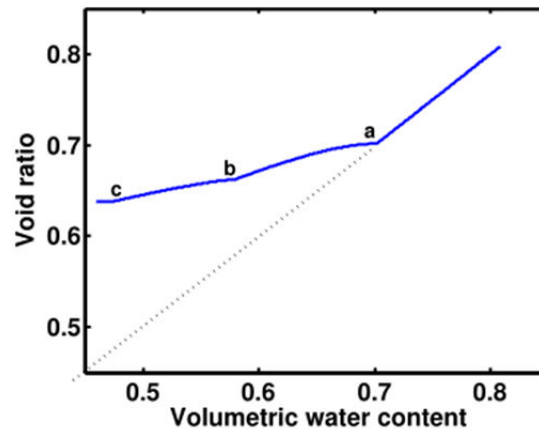


Fig. 8. Void ratio versus volumetric water content simulated.

CONCLUSIONS

The presented numerical modeling is based on a conceptual model with the intention to assess the different scenarios for air entry observed in the recent experiments and quantitatively evaluate the implications of these scenarios, leading to the development of different saturation regimes. Obviously the model can be improved if more complicated configurations are considered. However, even sophisticated numerical investigations with Discrete Element suffers from the lack of tools to account for transition of different saturation regimes and thus have to be confined to low degrees of saturation applicable for pendular regime only (e.g. Scholtes et al. 2009). The presented model is able to conceptually show the three regimes: capillary, funicular and pendular during a drying process.

Only one scenario of air entry is discussed in this paper, air entry at middle (intersection of large and small pore) first. However, it might occur first at boundary of large pore as shown in experimental observation at Fig. 1, numerically this is possible in the presented model, depending mainly on the stiffness and evaporation rate of small pores. If stiffness and evaporation is much lesser than the value taken during this modeling, air entry at the LP-SP intersection would occur later than at large pore boundary.

REFERENCES

- Brinker, C.J. and Scherer, G.W. 1990). *Sol-Gel Science: The Physics and Chemistry of Sol-Gel Processing*. Academic Press, San Diego.
- Chen., W.F. and Han, D.J. (1988). *Plasticity for Structural Engineers*. Springer-Verlag, New York.
- Childs, E. C. (1969). *An Introduction to the Physical Basis of Soil Water Phenomena*. Wiley-Interscience, London.

- Fredlund, D.G. and Rahardjo, H. (1993). *Soil Mechanics for Unsaturated Soils*. John Wiley & Sons, New York.
- Fung, Y.C. (1984). *Biodynamics: circulation*. Springer, New York.
- Hill, R. (1950). *The Mathematical Theory of Plasticity*. Oxford University Press, Oxford.
- Holtz, R.D., Kavcs, W.D. and Sheahan, T.C. (2012). *An Introduction to Geotechnical Engineering*, 2nd Edition, Prentice Hall, New Jersey.
- Hu, L.B., Peron, H. and Laloui, L. (2013a). “Desiccation shrinkage of non-clayey soils: multiphysics mechanisms and a microstructural model.” *Int. J. Numer. Anal. Methods Geomech.* 37(12): 1761-1781.
- Hu, L.B., Peron, H. and Laloui, L. (2013b). “Desiccation shrinkage of non-clayey soils: a numerical study.” *Int. J. Numer. Anal. Methods Geomech.* 37(12): 1782-1800.
- Hu, L.B., Peron, H., Hueckel, T. and Laloui, L. (2013c). “Mechanisms and critical properties in drying shrinkage of soils: experimental and numerical parametric studies.” *Can. Geotech. J.* 50(5): 536–549.
- Kodikara, J., Barbour, S.L., and Fredlund, D.G. (1999). “Changes in clay structure and behaviour due to wetting and drying.” *Proc. of the 8th Australia-New Zealand Conf. on Geomechanics*. Hobart, Australia, 179-185.
- Maeda, N., Israelachvili, J. N. and Kohonen, M. M. (2003). “Evaporation and instabilities of microscopic capillary bridges.” *Proc. National Academy of Sciences of the USA*. 100(3): 803-808.
- Mielniczuk, B., Hueckel, T. and El Youssoufi, M.S. (2013). “Micro-scale study of rupture in desiccating granular media.” *ASCE GSP 231: Geo-Congress 2013*, 808-817.
- Pellenq, R.J.M., Coasne, B., Denoyel, R.O. and Coussy, O. (2009). “Simple phenomenological model for phase transitions in confined geometry. 2. Capillary condensation/evaporation in cylindrical mesopores.” *Langmuir*. 25(3): 1393-1402.
- Peron, H. Hueckel, T., Laloui, L. and Hu, L. B. (2009). “Fundamental of desiccation cracking of fine grained soils: experimental characterization and mechanisms identification.” *Can. Geotech. J.* 46(10): 1177-1201.
- Puyate, Y.T. and Lawrence, C.J. (2006). “Sherwood’s models for the falling-rate period: A missing link at moderate drying intensity.” *Chem. Eng. Sci.* 61(21):7177-7183.
- Scholtès, L., Chareyre, B., Nicot, F. and Darve, F. (2009). “Discrete modelling of capillary mechanisms in multi-phase granular media.” *Computer Modeling in Engineering & Sciences*. 52(3): 297-318.
- Sherwood, T.K. (1929). “The drying of solids I.” *Ind. Eng. Chem.* 21(1): 12-14.
- Taylor, G.I. (1959). “The dynamics of thin sheets of fluid. III. Disintegration of fluid sheets.” *Proc. R. Soc. London, Ser. A*. 253(1274): 313-1959.
- Terzaghi K. (1927). “Concrete roads - A problem in foundation engineering.” *Journal of the Boston Society of Civil Engineers*. 14: 265-282.
- Urso, M.E.D., Lawrence, C.J. and Adams, M.J. (1999). “Pendular, funicular, and capillary bridges: results for two dimensions.” *Journal of Colloid and Interface Science*. 220(1): 42-56.

Numerical Studies on Filter of Piping in Broadly Graded Cohesionless Soils

Yanfeng Bai¹, Jian Zhou² and Zhixiong Yao³

¹Shanghai City Urban Construction Design and Research Institute, Shanghai, China, 200120; b6y6f6@163.com

²Department of Geotechnical Engineering, Tongji University, Shanghai, China, 200092; tjuzj@vip.163.com

³Fujian Communications Science Research Institute, Fuzhou, China, 350004; bearer@126.com

ABSTRACT: China is one of the countries that suffer from flood casualty severely, and piping disaster is catastrophic. To explore the piping mechanism, putting forward a valid piping prevention measure has great significance. Due to the complexity of piping, study on the mechanism is still in controversy although it has been on for more than one hundred years. Therefore, more precise analysis is required to clarify the filter prevention piping mechanisms. Because of comprehensive study on the documentations and generalizing the research founding of predecessors and their shortage, an analytical model taking the large deformation of medium and coupling of fluid and solid into account is established to simulate base soil-filter system during seepage in broadly graded cohesionless soils by using and developing PFC3D program based on discrete element method. The model shows that the key point of piping control is locating filter, and the factor between layers is important for the effectiveness of filter. The model predictions are also compared with the available empirical recommendations. On a series of base material, laboratory tests verify the validity of the model.

INTRODUCTION

Flood is very common in many countries including China. Dams have been built for flood control, irrigation works, recreation activities, and navigation. Dam failures are common and are caused by a multitude of factors, such as poor construction, inadequate design, piping, and improper maintenance. The phenomenon of piping is commonly observed under dams, and it involves subsurface erosion of soil particles piping which is a form of seepage erosion by referring to the development of subsurface channels in which soil particles are transported through porous media. Piping begins at the land-facing side of the structure where the flow lines converge. High seepage pressure may force a slit to develop; then the process of erosion

develops backward under the dam, and if the process continues, the structure may be undermined and collapse.

Much experimental and numerical work (Terzaghi 1939; U.S. Army 1971; Lafleur 1984; Lowe 1988; Indraratna et al. 1996) has been conducted to develop empirical filter criteria for various base soil-filter combinations. Probabilistic formulations have also been considered in the development of filter design criteria (Honjo and Veneziano 1985). However, limited studies are based on discrete element method.

In this paper, a coupled fluid-particle model based on PFC3D was given to modeling the behavior of filters for cohesionless base soil. The result is discussed and compared with laboratory test.

MODELING PROCEDURE

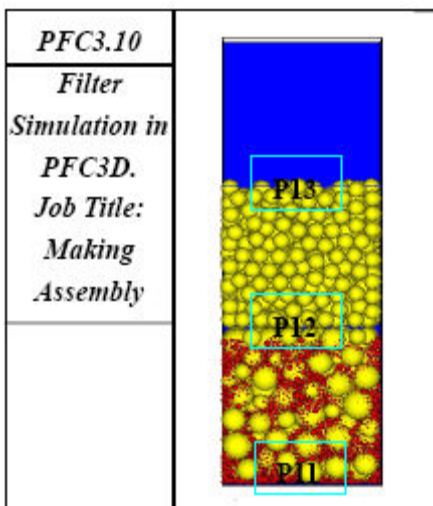


Fig. 1. Illustration of the PFC3D model

Fig. 1 shows the model of the initial state of the ball assembly and walls. The model consists of balls and surrounding walls, $0.02 \text{ m} \times 0.02 \text{ m} \times 0.04 \text{ m}$ (width \times depth \times height). The ball size distribution is 0.1-5 mm diameter. The sidewall of the model consists of four imperviousness rigid wall. At the top and bottom, mesh wall is used to represent permeable boundary, which could add hydraulic pressure, drainage and particle loss.

The generators of a center dense base soil in the space are stochastic, and then dropped by gravity. After reaching a steady state condition, filter which has a certain ball size distribution and thickness is generated at the top of the base soil, and then dropped by gravity until it reaches to a relatively natural state. Then full water to saturation and begin to original coupling calculation which could make it to initial whist water pressure state. When the imbalance forces eliminate little enough and the saturation sand sample basically satisfies whist water pressure state, boundary condition is given. At the bottom of the sample, a pressure of 2000Pa is given, at the same time, no pressure is put on the top of the sample, and there will be a head difference which could simulate upwards seepage. The sample is broadly graded

sand, the number of particle is large and the diameter is difference, so the speed of calculating is slowly. Considering the time, the principle of centrifuge test is used and the scale is 1:5.

The contact stiffness model uses the linear contact model. The slip model between particles uses the friction slip model. Table 1 shows the material properties.

Table 1. Material properties of the model

(Ball)		(Water)		
Diameter	0.1-5.0 mm	Density		1000 kg/m ³
		Viscosity		1.0×10 ⁻³ Pa.s
Density	2650 kg/m ³	Fluid cell	Volume	5×5×5 mm ³
Normal Stiffness	1.0×10 ⁶ N/m		Number	4×4×8
Shear Stiffness	1.0×10 ⁶ N/m	(Timestep)		
Friction Coefficient	0.5	TMC		6.71 × 10 ⁻⁸ s
(Wall)		TFC		5.05 × 10 ⁻⁵ s
Normal Stiffness	1.0×10 ⁶ N/m			
Shear Stiffness	1.0×10 ⁶ N/m			
Friction Coefficient	0.5			

RESULTS

Several groups of numerical sample with different factor between layers were produced, and the influence of coefficient between layers was analyzed. However, as a result of computation, the speed will be very slow if the number of the particles is large, the numerical modeling used uniform base soils and different filter to satisfy require of different coefficient between layers.

At the bottom of the sample, a pressure of 2000Pa was given. At the same time, no pressure was put on the top of the sample, and there will be a head difference. Hydraulic pressure was slowly given, and the time of calculating seepage was nearly two days. The analysis result shows that, particle loss fraction will be increased if coefficient between layers becomes bigger; however, the relationship is nonlinear. When coefficient between layers is near 3, although the calculating time of seepage is longer enough, the particle loss fraction is very small, only 3.53% and particle loss has a trend of convergence and stabilization. Under this condition, the pore of the filter is small enough to prevent the particle which could transfer the base lose, even if there is small part of particle lose, the big part of the particle which could transfer will jam the pore and form a self-sieve layer between base soil and filter, then the filter could be considered effective.

Table 2. Ultimately particle loss fraction with different coefficient between layers

D ₁₅ /d _{85s}	2.73	3.82	4.55	5.97	6.72	7.46	8.21
Particle loss fraction (%)	3.53	4.45	6.87	7.21	7.35	6.79	7.60

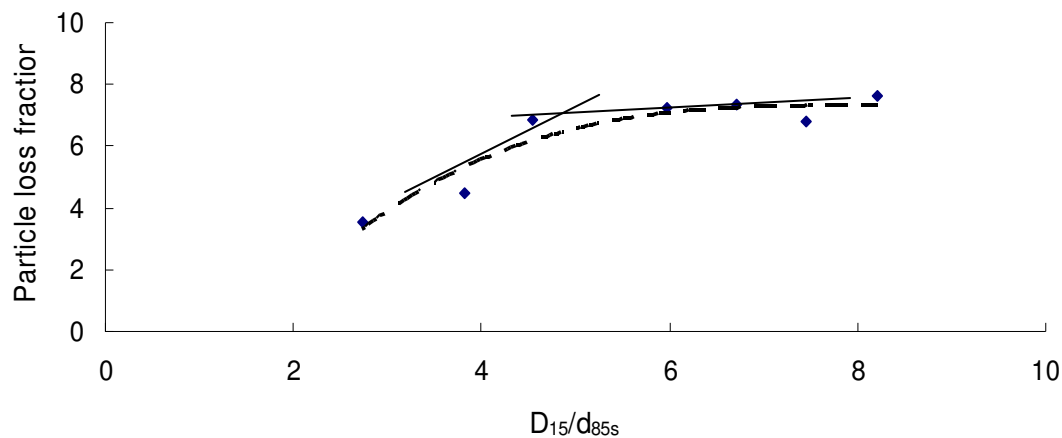


Fig. 2. Curve of D_{15}/d_{85s} and particle loss fraction

Fig. 2 shows that, coefficient between layers 5 is a critical point., when coefficient between layers is greater than 5, the particle loss fraction will became bigger and the fine particles will be loss entirely if time is enough..

The coefficient between layers is the key factor of the effective of the filter. If the filter particle is too large, the filter couldn't prevent losing of the particle, meanwhile, both the particle loss fraction and the porosity of the base soil become bigger distantly, so the filter becomes ineffective. The result shows that particle loss fraction is small and has a trend of stability when coefficient between layers is less than 4. When coefficient between layers is between 4 and 5, the filter is on the critical sate which detains the filter is effective or ineffective. When coefficient between layers is greater than 5, both the particle loss fraction and the porosity of the base soil will become bigger distinctly and has no trend of stability, the filter is ineffective.

COMPARISON WITH LABORATORY TESTS

To describe and test the validity of the model predictions, a comparison with a series of laboratory tests is described.

A large-scale filtration apparatus (500-mm long, 100-mm broad and 600-mm high) was constructed to investigate the filtration of coarse and noncohesive materials typical of the filter and drainage zones within embankment dams. The tests described here employed a series of broad-graded sands as the 100-mm thick base soil and well-graded gravel as the 100-mm-thick filter. Finer gravel was placed (approximately 10cm deep), as the flow buffer which can ensure flow is uniformity and avoid flow fling sample to destroy. The base soil was placed and lightly compacted in a single layer of 100 mm. The filter was placed and compacted in 50-mm layers. Erosion was induced by a uniform upward flow of 0.2kPa/min. The experiment was repeated for different base-filter combinations with varying filter retention ratios, D_{15}/d_{85s} . In this paper, filter and base-soil particle sizes are denoted by D and d , respectively. The result is shows in Tab. 3.

Table 3. Result of Laboratory test

sample	filter			Base soil			D_{15}/d_{85s}	i_c	Piping? (Y/N)
	Height (cm)	D_{15} (mm)	D_{min} (mm)	Height (cm)	d_{85s} (mm)	Cu			
F1	10	1.15	1	10	0.46	12.43	2.5	/	N
F2	10	1.94	1	10	0.46	9.47	4.2	/	N
F3	10	2.35	1	10	0.46	15.94	5.1	/	Little
F4	10	2.82	2	10	0.46	12.43	6.1	0.75	Little
F5	10	3.00	2	10	0.46	9.47	6.6	0.68	Y
F6	10	3.45	2	10	0.46	12.33	7.5	0.72	Y
F7	10	4.29	2	10	0.46	12.43	9.3	0.52	Y
F8	10	4.62	2	10	0.46	14.00	10.0	0.45	Y
F9	10	5.31	2	10	0.46	12.33	11.5	0.42	Y
F10	10	5.72	2	10	0.46	14.00	12.4	0.39	Y
F11	10	5.31	2	10	0.46	12.33	11.5	0.24	Y
F12	10	5.31	2	10	0.46	12.33	11.5	0.61	Y
F13	10	5.31	2	10	0.46	12.33	11.5	0.85	Y
F14	10	5.31	2	10	0.46	12.33	11.5	0.34	Y
F15	10	5.31	2	10	0.46	12.33	11.5	0.25	Y

The result shows that the filter is effective when coefficient between layers is smaller than 4. When coefficient between layers is between 4 and 5, the filter is on the critical state, detaining the effective or ineffective filter. When coefficient between layers is greater than 5, the filter is ineffective.

The model predicts similar trends to those observed in the laboratory.

CONCLUSIONS

By using and developing PFC3D program based on discrete element method, the analytical model taking the large deformation of medium and coupling of fluid and solid into account is established to simulate base soil-filter system during seepage in sandy soils. The comparison with laboratory results has shown that the current model predicts particle movement and capture which is similar to the measured data for broadly graded noncohesive base and filter materials. The model is able to predict other samples with different parameters.

ACKNOWLEDGMENTS

The research is supported by the Chinese National Natural Science Foundation, Grant numbers 50379037. This support is gratefully acknowledged.

REFERENCES

- C. S. P. Ojha and V. P. Singh. (2001). "Influence of Porosity on Piping Models of Levee Failure." *Journal of Geotechnical and Geoenvironmental Engineering*, Vol. 127(12):1071-1074.
- Honjo, Y., and Veneziano, D. (1989). "Improved filter criterion for cohesionless soils." *J. Geotech. Engrg.*, ASCE, Vol. 15(1), 75-83.
- Indraratna, B., Vafai, F., and Dilema, E. L. G. (1996). "An experimental study of filtration of a lateritic clay slurry by sand filters." *Proc., Inst of Civ. Engrs., Geotech. Engrg.*, London, England, Vol. 119(2), 75-83.
- Lafleur, J. (1984). "Filter testing of broadly graded cohesionless tills." *Canadian Geotech. J.*, Ottawa, Canada, Vol. 21(4), 634-643.
- Lowe, J. (1988). "Seepage analysis in advanced dam engineering for design, construction and rehabilitation." *New York: Van Nostrand Reinhold*, 270-275.
- Terzaghi, K. (1939). "Soil Mechanics a New Chapter in Engineering Science." *J. Institution of Civil Engineers*, London, Vol. 12, 106-141.
- U.S. Army. (1971). "Dewatering and groundwater control for deep excavations." *Tech. Memo. No. 5-818-5 (April)*, *Ofc. of Engrs.*, U.S. Army, Washington, D.C.

Multi-phase Mechanics of the Interaction between the Soil, Water, and Coastal Structure during the Tsunami Disaster

Imase Tatsuya¹, Maeda Kenichi², Miyake Michio³, Tsurugasaki Kazuhiro³ Sumida Hiroko³ and Sawada Yutaka⁴

¹Ph.D. student, Nagoya Institute of Technology, Gokiso-cho, Showa-ku, Nagoya 466-8555 Japan; cih18501@stn.nitech.ac.jp

²Professor, Nagoya Institute of Technology, Gokiso-cho, Showa-ku, Nagoya, Japan; maeda.kenichi@nitech.ac.jp

³Ph.D., Naruo Research Institute, Toyo Construction Co., Ltd, Naruohama, Nishinomiya-shi, Hyogo 663-8142 Japan; miyake-michio@toyo-const.co.jp

⁴Assistant Professor, Faculty of Agriculture, Kobe University, Rokkodai-cho, Nada-ku, Kobe 657-8501 Japan; sawa@harbor.kobe-u.ac.jp

ABSTRACT: A coastal area in the Tohoku district was fatally damaged by the Great Tohoku Earthquake that occurred in Japan. However, the mechanism of the tsunami disaster for the coastal structure has not yet been completely revealed. In this paper, we discuss the tsunami disaster and how the multi-scaling problems and multi-phase interactions among the soil and water affect structures. Based on centrifuge tests and smoothed particle hydrodynamics (SPH) simulations with Tsunami-soil-structure interactions, the breakwater caused destabilization by scouring the seabed soil, which was a result of the tsunami seepage flow, and consequently, the ground strength decreased. Therefore, a bearing-capacity failure may occur in a breakwater exposed to long-acting tsunami forces due to the decrease in the rigidity of the seabed soil.

INTRODUCTION

In Japan, a magnitude (Mw) of 9.0 earthquake occurred in 2011. Following this earthquake, a tsunami occurred and it struck the coastal area fronting the Pacific Ocean side from Hokkaido to Chiba Prefecture. This gigantic tsunami caused damage for many coastal structures. However, the mechanism of the tsunami disaster for the coastal structure has not yet been completely revealed. The establishment of measures to minimize damage is urgently required, and thus the situation and mechanism of the damage caused by the Great East Japan Earthquake must be elucidated as soon as possible. For example, the breakwater damage occurs due to the following causes besides tsunami force: (1) scour due to an overflow, and (2) scour around the breakwater. Based on these causes, the magnitude of a tsunami force and overflow, and also scour phenomenon should be considered as key factors. To examine tsunami external force and overflow, precious data newly obtained through the Great East